Comparison of Levels of Electronic Structure Theory in Direct Dynamics Simulations of C 2 H 5 F → HF + C 2 H 4 Product Energy Partitioning †

ARTICLE *in* THE JOURNAL OF PHYSICAL CHEMISTRY A · FEBRUARY 2006

Impact Factor: 2.69 · DOI: 10.1021/jp052888p · Source: PubMed

4 AUTHORS, INCLUDING:

Kihyung Song
Korea National University of Education
99 PUBLICATIONS **2,579** CITATIONS

SEE PROFILE

Comparison of Levels of Electronic Structure Theory in Direct Dynamics Simulations of $C_2H_5F \rightarrow HF + C_2H_4$ Product Energy Partitioning†

Eunjung Dong,‡ Donald W. Setser,§ William L. Hase,|| and Kihyung Song*,‡

Department of Chemistry, Korea National University of Education, Chongwon, Chungbuk 363-791 Korea, Department of Chemistry, Kansas State University, Manhattan, Kansas 66506-3701, and Department of Chemistry and Biochemistry, Texas Tech University, Lubbock, Texas 79409-1061

Received: May 31, 2005; In Final Form: July 27, 2005

Direct dynamics simulations at the MP2/6-311++G** level of theory were performed to study $C_2H_5F \rightarrow HF + C_2H_4$ product energy partitioning. The simulation results are compared with experiment and a previous MP2/6-31G* simulation. The current simulation with the larger basis set releases more energy to HF vibration and less to $HF + C_2H_4$ relative translation as compared to the previous simulation with the 6-31G* basis set. The HF rotation and vibration energy distributions determined from the current simulation are in overall very good agreement with previous experimental studies of C_2H_5F dissociation by chemical activation and IRMPA. A comparison of the simulations with experiments suggests there may be important mass effects for energy partitioning in HX elimination from haloalkanes. The transition state (TS) structures and energies calculated with MP2 and the 6-31G* and 6-311++G** basis sets are compared with those calculated using CCD, CCSD, CCSD(T), and the 6-311++G** basis set.

I. Introduction

In a recent study,[1] an ab initio direct dynamics trajectory simulation, at the MP2/6-31G* level of theory, was used to determine product energy partitioning for the four-centered elimination of HF from vibrationally excited C_2H_5F. This is a particularly interesting system to study, since the vibrational and rotational energies of the HF product have been measured.[2−4] In addition, analyses of the experiments have been used to correlate product energy partitionings for hydrogen halide, i.e., HX, eliminations from different halo-carbon molecules.[3] The vibrational and rotational energies of the HF product determined from the simulations[1] are in very good agreement with experiment. The populations of the HF vibration states decrease monotonically, as determined from experiments,[3] with the populations for the low- and high-energy vibration states somewhat larger and smaller, respectively, than the experimental results. The HF rotational temperature is in excellent agreement with experiment.[2]

To analyze product energy partitioning for unimolecular dissociation reactions, the total energy available to the reaction products is often divided into two parts,[3] i.e., the excess energy at the dissociation TS and the potential energy released in the exit channel (the exit-channel potential energy barrier). With such an analysis, very poor agreement was found with proposed values[3] for partitioning of the $C_2H_5F \rightarrow HF + C_2H_4$ exit-channel potential energy barrier to the individual product energies,[1] in contrast to the quite good agreement with experiment for partitioning of the total energy available to the HF rotation and vibration. From the simulations, the release of the potential energy barrier is 81%, <0.05%, 5%, 11%, and 3% to relative translation, C_2H_4 vibration, C_2H_4 rotation, HF vibration, and HF rotation, respectively. This result is substantially different than the deduction from experiment,[3] which summarizes the potential energy release as 20%, 45%, 24%, and <12% to relative translation, C_2H_4 vibration and rotation, HF vibration, and HF rotation. The striking difference between these two energy partitionings is that the simulations predict that the vast majority of the exit-channel potential is released to product translation with negligible partitioning to C_2H_4 vibration, while analysis of the experiments suggests that C_2H_4 vibration and rotation is the principal recipient of the potential release, with a much smaller partitioning to relative translation.

It is important to determine the origin(s) of the difference in the partitioning of the $C_2H_5F \rightarrow HF + C_2H_4$ exit-channel potential energy release found from the trajectory simulations as compared to that given by the model deduced from experiments.[1] One issue which should be investigated is the accuracy of the MP2/6-31G* theory used for the direct dynamics simulations. This level of theory gives an accurate potential energy barrier, i.e., only 2 kcal/mol lower than the experimental value. However, the larger 6-311++G** basis set gives some differences in the intrinsic reaction coordinate (IRC) potential, and the $[C_2H_4\text{- - -HF}]^‡$ transition state's structure and vibrational frequencies as compared to what is found with the smaller 6-31G* basis.[1] It is of interest to determine if these differences affect the calculated product energy partitioning.

In the work presented here, the product energy partitioning for $[C_2H_4\text{- - -HF}]^‡ \rightarrow HF + C_2H_4$ dissociation is determined with direct dynamics and the MP2/6-311++G** theory, and compared with the previous MP2/6-31G* results. In addition, the $[C_2H_4\text{- - -HF}]^‡$ transition state structure and potential energy are calculated with the CCD, CCSD, and CCSD(T) theories and the 6-311++G** basis set and compared with the previous results determined using MP2/6-31G* and MP2/6-311++G**. These comparisons provide insight into the sensitivity of the reaction's potential energy surface to the level of electronic structure theory and the size of the basis set.

† Part of the special issue "William Hase Festschrift".

* Corresponding author: Kihyung Song. Email: ksong@pchem.knue.ac.kr.
‡ Korea National University of Education.
§ Kansas State University.
|| Texas Tech University.

10.1021/jp052888p CCC: $33.50
Published on Web 09/13/2005

TABLE 1: C_2H_4−HF‡ Transition State Structure at Different Levels of Electronic Structure Theory[a]

	geometry[b]					
theory	*R*(C−H)	*R*(C−C)	*R*(C−F)	*R*(H−F)	∠H−C−C	∠F−H−C
MP2/6-31G*	1.367	1.398	1.865	1.242	73.6	132.8
MP2/6-311++G**	1.321	1.404	1.883	1.290	73.2	135.3
CCD/6-311++G**	1.313	1.406	1.903	1.289	73.9	135.9
CCSD/6-311++G**	1.308	1.409	1.921	1.297	74.6	135.9

[a] The calculations were performed with frozen-core basis sets. [b] Distances are in angstroms and angles in degrees.

II. Computational Procedure

The calculations were performed at the Korea National University of Education using the same procedures as described in the previous article which reports the MP2/6-31G* direct dynamics simulations of $[C_2H_4\text{- - -HF}]^{\ddagger} \rightarrow HF + C_2H_4$ product energy partitioning.[1] The electronic structure calculations were performed with the *Gaussian 03* computer program.[5] The direct dynamics simulations were carried out with the VENUS[6]/*Gaussian*[5] package of computer programs. To calculate the product energy partitioning, the trajectories were initiated at the $[C_2H_4\text{- - -HF}]^{\ddagger}$ transition state, with initial energies selected from a microcanonical ensemble of states, and directed toward products. The role of the direct dynamics trajectories is to determine how the microcanonical ensemble of states at the TS is transformed into the nonstatistical energy distributions of the $HF + C_2H_4$ products.[7] A quasiclassical normal-mode model was used to select initial conditions for the TS microcanonical ensemble of states.[8,9] Standard algorithms in VENUS[6] were used to calculate the vibrational and rotational energies of the C_2H_4 product. The rotational quantum number J of the HF product was determined by equating its angular momentum j to $\sqrt{J(J+1)}\hbar$. The HF vibrational quantum number was determined by applying Einstein−Brillouin−Keller (EBK)[10] quantization to the HF internal energy

$$E_{HF} = p_r^2/2\mu + V(r) + j^2/2\mu r^2 \qquad (1)$$

The binning procedure was used to determine integer values for the J and n quantum numbers; e.g., all EBK values of n between −0.5 and 0.5 are identified with the $n = 0$ quantum level.

To directly compare with experiment, a simulation was performed with a TS vibration and reaction coordinate translational energy $E_{vt}^{\ddagger}$ of 42 kcal/mol above the zero-point level, i.e., the same $E_{vt}^{\ddagger}$ as for the experiments by Setser and co-workers.[3] To further analyze the product energy partitioning, additional simulations were performed for $E_{vt}^{\ddagger}$ of 32 and 3.45 kcal/mol. The HF rotational and vibrational energy distributions calculated for $E_{vt}^{\ddagger}$ of 32 kcal/mol may be compared with those measured by Quick and Wittig[2] in infrared multiphoton dissociation of C_2H_5F. This experiment technique is thought to dissociate C_2H_5F molecules with modest excess energies.[2] For each of the simulation studies, *RT*/2 (300 K) of rotational energy was added to each of the TS's rotation axes. Each trajectory contains zero-point energy (ZPE) in the vibrational modes orthogonal to the reaction coordinate, and the $E_{vt}^{\ddagger}$ of 42 and 32 kcal/mol are distributed randomly between the TS's vibrational and reaction coordinate degrees of freedom using microcanonical sampling.[8,9] For the calculations with $E_{vt}^{\ddagger} = 3.45$ kcal/mol, all of this energy was added to reaction coordinate translation. A total of 223, 148, and 100 trajectories were calculated for $E_{vt}^{\ddagger}$ of 42, 32, and 3.45 kcal/mol, respectively.

TABLE 2: Angle between the CH_2 Plane and C−C Bond at the TS

	angles (degrees)	
theory	α, H-side[a]	α, F-side[b]
MP2/6-31G*	156.5	167.2
MP2/6-311++G**	157.8	168.4
CCD/6-311++G**	156.1	170.5
CCSD/6-311++G**	155.3	171.3

[a] This is the angle between the CH_2 plane and the C−C bond for the end of the molecule the H-atom is departing. [b] Same as a, but the end of the molecule the F-atom is departing.

III. Computational Results

A. Electronic Structure Calculations. Geometries of the $[C_2H_4\text{- - -HF}]^{\ddagger}$ TS calculated at different levels of electronic structure theory are compared in Table 1. The MP2, CCD, and CCSD theories, with the 6-311++G** basis set, all give similar geometries for the $[C_2H_4\text{- - -HF}]^{\ddagger}$ TS. Their lengths for the rupturing C−H bond and forming H−F bond are shorter and longer, respectively, than the MP2/6-31G* values, indicative of an earlier TS[11,12] than that of MP2/6-31G* theory. Interestingly, these differences in the early/late TS characteristics are not present in the C−C bond length, which is nearly the same for all the levels of theory. Models of product energy partitioning[3,4,11,12] suggest that the shorter C−H and longer H−F bond lengths of the MP2/6-311++G** TS should result in more energy release to product HF vibration, and as shown below, this is indeed found from the direct dynamics simulations. Product energy partitioning may also be affected by the degree to which the C_2H_4 moiety of the TS is nonplanar. This property is considered in Table 2 where α, the angle between the CH_2 plane and the C−C bond, is listed for both ends of the TS. Similar extents of nonplanarity are found for both basis sets and all three levels of theory. For the F-side of the TS, α is only ∼10° from planarity. For the H-side, α is substantially different, i.e., ∼25° less than 180°. Overall, the MP2 and CCSD calculations, with the 6-311++G** basis set, give TS structures in good agreement. The most substantial difference in the TS structures is the 0.04 Å longer C−F bond for CCSD.

Energies for the $[C_2H_4\text{- - -HF}]^{\ddagger} \rightarrow HF + C_2H_4$ reaction at the different levels of electronic structure theory are listed in Table 3. The MP2 and CCSD(T) theories, with the 6-311++G** basis set, give similar electronic energies for the TS and the products, resulting in similar values for the exit-channel potential energy barrier release. The MP2 and CCSD(T) values for this potential energy release are 50.00 and 51.00 kcal/mol, respectively. These are classical barriers, without a zero-point energy correction, and including this correction with the MP2/6-311++G** vibrational frequencies raises the barrier by 0.62 kcal/mol.[1] The MP2 and CCSD(T) values for the barrier, with the 6-311++G** basis set, are in excellent agreement with the experimental value of 49.0 ± 2 kcal/mol.[3] The classical MP2/6-31G* barrier is 44.88 kcal/mol and approximately 5 kcal/mol lower than the MP2 and CCSD(T) barriers with the 6-311++G** basis set.

TABLE 3: $C_2H_5F^{\pm} \rightarrow HF + C_2H_4$ Energies[a]

theory	molecular energies (au)			
	$C_2H_5F^{\pm}$	HF	C_2H_4	E_r (kcal/mol)[b]
MP2/6-31G*	−178.4069299	−100.1841614	−78.2942851	44.88 (45.33)
MP2/6-311++G**	−178.6022099	−100.2979372	−78.3839526	50.00 (50.62)
CCD/6-311++G**	−178.5618557	−100.2791231	−78.3816939	55.82 (56.44)
CCSD/6-311++G**	−178.569464	−100.2807864	−78.3742919	53.72 (54.34)
CCSD(T)/6-311++G**	−178.5898871	−100.2850638	−78.3860909	51.00 (51.62)

[a] The calculations were performed with frozen-core basis sets. [b] E_r is the exit channel classical reverse potential energy barrier without zero-point energy corrections. The barriers with zero-point energy corrections are given in parentheses. The experimental barrier is 49.0 ± 2.0 kcal/mol.

TABLE 4: Average Product Energy Partitioning for MP2/6-31G* and MP2/6- 311++G Direct Dynamics[a]**

product energy	$E_{vt}^{\ddagger}$=	MP2/6-31G* [b]			MP2/6-311++G** [c]		
		3.45	27	42	3.45	32	42
rel trans		75.4	56.8	49.7	67.8(1.2)[d]	48.2(1.0)	46.2(1.0)
C_2H_4 vib		6.1	24.2	31.5	6.8(0.7)	26.2(0.8)	29.3(0.6)
C_2H_4 rot		4.6	5.9	6.0	5.1(0.3)	5.5(0.3)	6.2(0.3)
HF vib		10.5	8.7	7.9	16.9(1.3)	15.8(1.1)	14.0(1.0)
HF rot		3.4	4.4	4.9	3.4(0.3)	4.3(0.4)	4.3(0.3)

[a] The average energy partitioning is given in percent. In addition to the TS's vibration/reaction coordinate translation energy $E_{vt}^{\pm}$, the TS also contains 3*RT*/2 rotation energy (T = 300 K). Energies are given in kcal/mol. Zero-point energy is not included in the C_2H_4 and HF vibration energies. [b] For the MP2/6-31G* simulations, 1000, 300, and 400 trajectories were calculated at $E_{vt}^{\ddagger}$ of 42, 27, and 3.45 kcal/mol, respectively; see ref 1. [c] For the MP2/6-311++G** calculations, 223, 148, and 100 trajectories were calculated at $E_{vt}^{\ddagger}$ of 42, 32, and 3.45 kcal/mol, respectively. [d] The uncertainty, in parentheses, is the standard deviation of the mean.

B. Direct Dynamics Simulations. *1. Product Energy Distributions.* The average product energy partitionings determined from the MP2 simulations with the 6-31G* and 6-311++G** basis sets are compared in Table 4. Uncertainties are listed for the 6-311++G** basis set results, and they are quite small. The uncertainties are even smaller for the 6-31G* results, since more trajectories were calculated. The total energy available to the reaction products is

$$E_{av} = E_r^{\circ} + E_{vt}^{\ddagger} + E_r^{\ddagger} \qquad (2)$$

where E_r° is the classical potential energy difference between the TS and products, with the TS and products ZPE difference included, $E_{vt}^{\ddagger}$ is TS's vibration and reaction coordinate translational energy, and $E_r^{\ddagger}$ = 3*RT*/2 is the TS's rotational energy. The patterns for product energy partitioning given by the two basis sets are similar. Of particular interest are the partitionings to HF rotation and vibration, since these are the two product energies which have been measured experimentally. The major difference between the two sets of results is that the 6-311++G** basis partitions less energy to relative translation and more to HF vibration. The partitionings to the other degrees of freedom are nearly the same for the two simulations. Relative translation is the principal recipient of the available energy at each of the $E_{vt}^{\ddagger}$, with C_2H_4 vibration also becoming an important recipient at high $E_{vt}^{\ddagger}$.

Distributions of the different product energies, for the 6-311++G** basis set simulations, have the same overall forms and shapes as reported previously[1] for the 6-31G* basis set simulations. The distributions $P(n)$ of the populations of the HF vibrational states for the 6-311++G** simulations are shown in Figure 1. The $P(n)$ for $E_{vt}^{\ddagger}$ of 3.45 and 42 kcal/mol are compared with those previously reported for the 6-31G* simulations. The simulations with the 6-311++G** basis set gives lower population of the n = 1 state and higher populations of the n > 2 states as compared to the 6-31G* simulations. As shown in Table 4, the simulation with the larger basis set partitions 6% more of the available energy to the HF vibration.

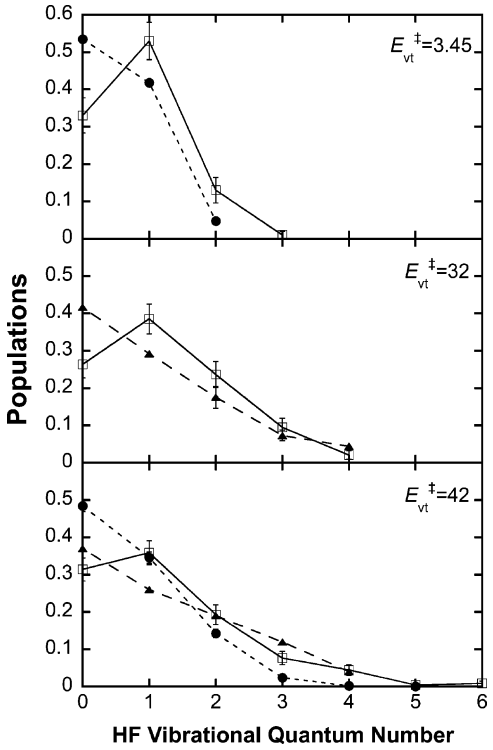

Figure 1. Populations of the HF vibrational states for $C_2H_5F \rightarrow HF + C_2H_4$ dissociation, with different amounts of vibration/reaction coordinate energy $E_{vt}^{\ddagger}$ in the $C_2H_5F^{\ddagger}$ transition state. □, results of the MP2/6-311++G** simulations; ●, results of the MP2/6-31G* simulations from ref 1; and ▲, experimental results. The experimental results for $E_{vt}^{\ddagger}$ of 32 and 42 kcal/mol are from refs 2 and 3, respectively.

Rotational temperatures of 940, 1806, and 2023 K are found when the average HF rotational energy, for the MP2/6-311++G** simulations at $E_{vt}^{\ddagger}$ of 3.45, 32, and 42 kcal/mol, is equated to *RT*. Similar rotational temperatures of 856, 1610, and 2164 K are found from the average HF rotational energies for the previous MP2/6-31G* simulations at $E_{vt}^{\ddagger}$ of 3.45, 27, and 42 kcal/mol. The MP2/6-311++G** simulated probability of the HF rotational quantum number J is approximated by the Boltzmann probability distribution

$$P(J) = (2J + 1)\, e^{-E_J/kT} \qquad (3)$$

The fits to the simulated $P(J)$ distributions are shown in Figure 2, where the fitted temperatures are 1134, 1782, and 1643 K for $E_{vt}^{\ddagger}$ of 3.45, 32, and 42 kcal/mol, respectively. Given the uncertainties in the simulated distributions, the fits may only be identified as approximate. This is exemplified by the different temperatures found from these fits as compared to those given

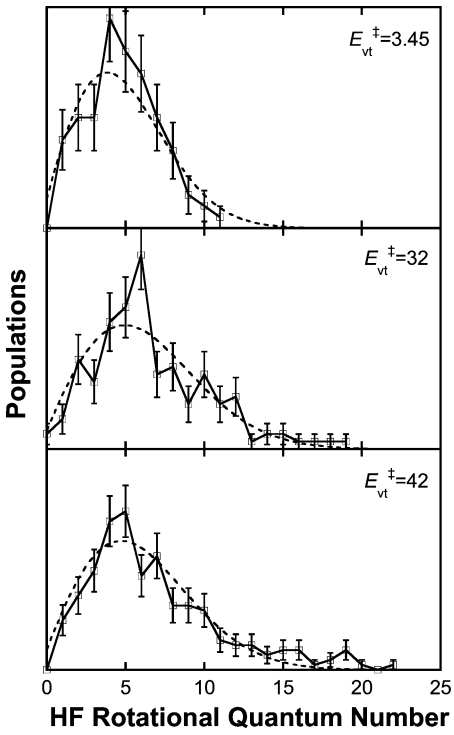

Figure 2. Populations of the HF rotational states for $C_2H_5F \rightarrow HF + C_2H_4$ dissociation with different amounts of vibration/reaction coordinate energy $E_{vt}^{\ddagger}$ (kcal/mol) in the $C_2H_5F^{\ddagger}$ transition state. The (□) points are the results of the MP2/6-311++G** simulations, and the (- - -) line is the fit to the Boltzmann distribution as described in the text.

above for the average HF rotational energy. It is possible that a Boltzmann $P(J)$ would emerge if the statistics of the simulations were refined by calculating more trajectories. However, for the MP2/6-31G* simulations,[1] for which up to 1000 trajectories were calculated for a specific $E_{vt}^{\ddagger}$, small, distinct non-Boltzmann components are seen in the simulated $P(J)$.[1] The temperatures determined from fits to the $P(J)$ distributions, for the MP2/6-31G* simulations at $E_{vt}^{\ddagger}$ of 3.45, 27, and 42 kcal/mol, are 764, 1373, and 1744 K and considerably different than those found from the $P(J)$ for the MP2/6-311++G** simulations. These differences my result in part from the poor statistics of the $P(J)$ distributions, particularly for the 6-311++G** simulations. However, non-Boltzmann characteristics for the $P(J)$ distributions may also contribute to this difference. The conclusion reached is that the 6-31G* and 6-311++G** basis sets, when used with MP2 theory, give similar HF rotational energy distributions, which appear to have distinct non-Boltzmann components.

2. Relationships between the TS Energy and the Product Energy Partitioning. The total internal energy $E^{\ddagger}$ of the TS for each simulation is the TS's vibration and reaction coordinate translation energy $E_{vt}^{\ddagger}$ plus its average rotational energy of $3RT/2 = 0.89$ kcal/mol. The total energy available to the products is $E^{\ddagger}$ plus the potential energy release E_r° in moving from the TS to the products, which is 50.62 kcal/mol for MP2/6-311++G** calculations. Zamir and Levine[13] suggested that the average value for each type of product energy $\langle E_i \rangle$ and the TS total energy $E^{\ddagger}$ have the linear relationship

$$\langle E_i \rangle = E_i^{\circ} + a_i E^{\ddagger} \qquad (4)$$

where the a_i give the fractions of $E^{\ddagger}$ partitioned to the different

TABLE 5: Parameters Describing the Partitioning of the Excess Energy and the Potential Energy Release[a]

	6-31G*		6-311++G**	
	a_i	E_i°/E_r°	a_i	E_i°/E_r°
rel trans	0.17	0.81	0.14	0.73
C_2H_4 vib	0.64	0.00	0.62	0.02
C_2H_4 rot	0.076	0.05	0.074	0.05
HF vib	0.046[b]	0.11	0.11	0.18
HF rot	0.067[b]	0.03	0.055	0.03

[a] a_i represents the fraction of the excess energy at the TS partitioned to a particular type of energy. $E_i^{\circ}/E_r^{\circ}$is the fraction of exit-channel potential energy release partitioned to a particular type of energy. [b] In the text of ref 1, these values are switched.

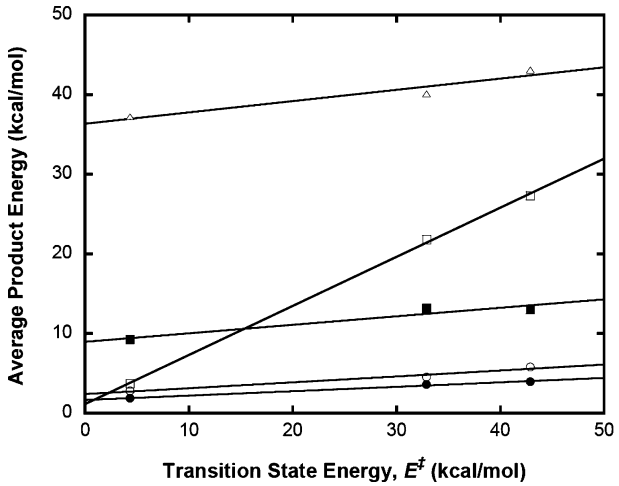

Figure 3. The average product energy in relative translation (△), C_2H_4 vibration (□), C_2H_4 rotation (○), HF vibration (■), and HF rotation (●). The transition state energy is the energy in excess of the zero-point energy level of the transition state, including the rotation energy $3RT/2$ at $T = 300$ K. The straight lines are the fits with eq 4.

product energies and the E_i° give the parts of E_r° which go to the different product energies. Summing eq 4 over i gives

$$\sum \langle E_i \rangle = \sum E_i^{\circ} + E^{\ddagger} \sum a_i \qquad (5)$$

where the sum of the a_i equals unity. The ratio E_i°/E_r° is the fraction of the exit-channel potential energy release, E_r°, partitioned to product energy i.

Equation 4 was found to give an excellent fit to the product energy partitioning for the MP2/6-31G* simulations,[1] and the resulting values for a_i and E_i°/E_r° are listed in Table 5. As shown in Figure 3, eq 4 also gives an adequate fit to MP2/6-311++G** simulation results reported here. (A better test of the adequacy of a linear fit would involve calculating the energy partitioning at additional values of $E^{\ddagger}$ and calculating more trajectories for each E_i to reduce the uncertainties in $\langle E^{\ddagger} \rangle$.) The fitted values are listed in Table 5, where they are compared with those for the previous 6-31G* simulation. Overall, the fitted parameters for the two basis sets are in very good agreement, with the only substantial differences for relative translation and HF vibration. The 6-31G* a_i values for relative translation and HF vibration are 0.03 and 0.06 larger and smaller than their 6-311++G** counterparts, respectively. The differences in the E_i°/E_r° are somewhat larger, with the 6-31G* values for relative translation and HF vibration 0.08 and 0.07 larger and smaller, respectively.

It has been suggested that the TS's statistical distribution of energy is maintained as the reactive system moves from the TS to products.[14] The a_i values in eq 4 are fixed by the distribution of the excess energy at the TS, and this distribution

is assumed to be unaffected by the dynamics as the ensemble of trajectories moves from the TS to products. Thus, the model predicts the same set of a_i values for the 6-31G* and 6-311++G** simulations, since both sample the same energy distribution at the TS. The results in Table 5 are consistent with this model except for HF vibration, whose 6-311++G** a_i is a factor of 2 larger. Given the statistical uncertainties in the product energy partitionings (see Table 4), there are no significant differences in the a_i for relative translation or for the other product energies. The different a_i values for HF vibration indicates that the statistical distribution at the TS may be perturbed by the exit-channel dynamics. This is discussed in more detail in the Summary.

A difficulty in applying the statistical model is correlating vibration and reaction coordinate degrees of freedom in the TS with the products' external rotation and relative translation degrees of freedom. In addition, the partitioning of energy to relative translation and product rotation is dependent on angular momentum constraints and couplings as the molecule dissociates.[12,15] Orbital angular momentum may be conserved in moving from the TS to products, transforming into relative translation,[12] or it may couple statistically with product rotational angular momentum[16] and possibly other degrees of freedom. Such angular momentum constraints and couplings are components of statistical models for unimolecular decomposition and bimolecular association.[16−18] According to the simplest statistical model, the 18 vibration and reaction coordinate degrees of freedom of the TS correlate to 12 C_2H_4 vibration, 1 and 2 HF vibration and rotation, and 3 relative translation degrees of freedom. For the classical version of this model, $^{12}/_{18} = 0.67$ and $^{1}/_{18} = 0.056$ of $E_{vt}^{\ddagger}$ is partitioned to C_2H_4 and HF vibration, respectively. This value for C_2H_4 vibration is in very good agreement with the two direct dynamics a_i values of 0.64 and 0.62, which are the same within statistical uncertainties (see Table 4). On the other hand, the 6-31G* and 6-311++G** values of a_i for HF vibration are 0.046 and 0.11 and are different, with the former close to the statistical model value of 0.056. In previous work, Arunan et al.[3] used a quantum statistical model to partition $E_{vt}^{\ddagger}$ and determined 0.046 for a_i, which is identical to the 6-31G* result. The direct dynamics a_i values for relative translation are similar, i.e., 0.17 and 0.14, and agree with the classical statistical prediction of $^{3}/_{18}$, which is 0.17.

3. Correlation Between HF Vibration and Rotation Energies. The presence of any correlation between the initial HF $P(n)$ and $P(J)$ distributions, before any collisional relaxations, was investigated in the previous MP2/6-31G* direct dynamics simulation for $E_{vt}^{\ddagger} = 42$ kcal/mol.[1] Within the statistics of the simulation, the $P(J)$ were found to be same for the $n = 0$ and $n = 1$ vibrational levels. However, as n was increased beyond 1, there was a small decrease in the HF rotational energy and, thus, a weak correlation between HF vibration and rotation. Table 6 lists the average HF rotational energy versus HF vibrational state n for the MP2/6-311++G** simulations performed. Results are given for each of the $E_{vt}^{\ddagger}$ investigated. The average values of the HF rotational energy decrease with increase in n, indicating an inverse correlation between the HF vibrational and rotational energies. However, if the statistical uncertainties of the rotational energy are included, the inverse correlation remains, but is weak. More trajectories and better statistics are required to clearly identify the strength of this inverse correlation.

4. Comparison with Experiment. The results of the simulations may be compared with experimental measurements of the rotation and vibration energies of the HF product[2,3] and with a model deduced for partitioning the potential energy release to different product energies.[3] The latter results from summarizing experimental studies of HX elimination. Experiments by Setser and co-workers[3], for $C_2H_5F \rightarrow$ HF and C_2H_4 decomposition at $E_{vt}^{\ddagger} = 42$ kcal/mol, show that 15% of the available energy is partitioned to HF vibration. As shown in Table 4, the MP2/6-311++G** HF vibration energy partitioning of 14% is in excellent agreement with experiment, while the 6-31G* calculation underestimates the HF vibration energy. The populations of the HF vibration states $P(n)$, found from the simulations, are compared with experiment in Figure 1. Though these are some small differences, overall the simulation with the 6-311++G** basis set gives a $P(n)$ in good agreement with the experiments of Setser and co-workers. On the other hand, the 6-31G* calculations do not adequately populate the higher HF vibrational states.

TABLE 6: Average HF Rotational Energy for Different HF Vibrational Levels

	TS energy $E_{vt}^{\ddagger}$ [a]		
n[b]	3.45	32	42
0	2.3 (0.3)	4.0 (0.6)	4.3 (0.5)
1	1.7 (0.2)	4.3 (0.6)	4.0 (0.6)
2	1.7 (0.3)	2.8 (0.5)	3.3 (0.6)
3	0.4[c]	2.63 (0.6)	5.3 (1.6)

[a] The TS energy is in kcal/mol. The uncertainty, in parentheses, is the standard deviation of the mean. [b] n is the HF vibrational level. [c] The number of trajectories with this value of n is too small (only 1) to determine a meaningful $\langle E_{rot} \rangle$.

$P(n)$ has also been measured for C_2H_5F molecules dissociated by infrared multiple photon absorption (IRMPA).[2] These experiments are thought to dissociate C_2H_5F with energies in the range 20−35 kcal/mol, and in Figure 1, the measured $P(n)$ is compared with the simulated $P(n)$ for $E_{vt}^{\ddagger} = 32$ kcal/mol. The $n = 0$ population is not measured in the experiments, and in the presentation of the experimental results,[2] the population of $n = 1$ is estimated as 70% of that for $n = 0$. This $P(1)/P(0)$ relative population was obtained from related experiments.[19,20] Sirkin and Berry[19] estimated the ratio as 0.8 from experiments for CF_3CH_3. In previous work, Arunan et al.[3] used $P(1)/P(0) = 0.7$ as an average of the experimental results[19,20] of 0.8 ± 0.2 for $CH_2F + CH_3$ and 0.6 ± 0.2 for $H + CH_2CH_2F$. $P(1)/P(0) = 0.7$ is used here to represent the IRMPA data. As shown in Figure 1, the simulations at $E_{vt}^{\ddagger} = 32$ kcal/mol give a $P(n)$ distribution in very good overall agreement with the results of the experiments. The major difference between the simulations and experiments is that the simulations give an inverted $P(1)/P(0)$ ratio of 1.4 ± 0.3 compared to the value of 0.7 used for the experiments, as described above. The results of the simulation are in quite good agreement with experiment for the $n \geq 2$ levels.

In experiments of C_2H_5F dissociation by IRMPA, the distribution $P(J)$ of the HF rotation quantum number J is found to be Boltzmann with a temperature of 800 K.[2] The populations of the HF states are determined by infrared fluorescence, and at the 0.2 Torr pressure used in the experiments, there is some collisional relaxation of the nascent $P(J)$ which will have a higher temperature. The nascent distribution may also have some non-Boltzmann features as discussed above for the $P(J)$ determined from the simulations. Thus, 800 K is expected to be a lower limit to the true rotational temperature. The average excess energy of C_2H_5F molecules dissociated in the IRMPA experiments is thought to lie between 20 and 35 kcal/mol. For $E_{vt}^{\ddagger} = 32$ kcal/mol and the MP2/6-311++G** simulations

reported here, the temperature determined from the fit to the $P(J)$ distribution is 1782 K and the temperature from the average HF rotational energy is 1806 K. For the MP2/6-31G* simulations, the respective temperatures are 1373 and 1610 K. Though there are differences in the 6-31G* and 6-311++G** rotational temperatures, both sets are definitely higher than the 800 K used to fit the experiments, suggesting there is some collisional relaxation of the initial $P(J)$ distribution as suggested by Quick and Wittig.[2]

As shown in Table 6, a weak inverse correlation is found between the HF vibration and the rotation energies for the MP2/6-311++G** simulations. A similar weak correlation was found in the previous MP2/6-31G* simulations. However, in analyzing the product energy distributions, for the IRMPA experiments of C_2H_5F dissociation, it is assumed the P(J) distribution and, thus, HF rotational temperature is the same for each of the HF vibrational states n.[2] Thus, there is no correlation between the J and n distributions. An absence of a correlation may in part arise from collisional relaxation of the nascent P(J) distribution as described above.[2] Setser and co-workers[3] also found no correlation between the J and n distributions for HF elimination from C_2H_5F, but collisional relaxation also occurs in their experiments. On the other hand, an inverse correlation between HF vibration and rotation was observed for CF_3CH_3 dissociation,[3] which forms HF with a much larger rotational energy. The strong suggestion is that collisional relaxation of the relatively low energy J states formed during HF elimination from C_2H_5F precludes any observation of a weak initial inverse correlation between n and J.

As discussed in the Introduction, in an attempt to summarize a series of HX elimination reactions, it has been suggested that, for $C_2H_5F \rightarrow HF + C_2H_4$ dissociation, the partitioning of the exit-channel potential energy is 20%, 45%, 24%, and <12% to relative translation, C_2H_4 vibration and rotation, HF vibration, and HF rotation.[3] As shown in Table 1, the results of the earlier MP2/6-31G* simulations are strikingly different from this predicted energy partitioning. A similar difference is found for the MP2/6-311++G** simulations reported here. This simulation partitions less of the exit-channel barrier to relative translation and more to HF vibration than does the simulation with the smaller basis set. However, for both simulations, the partitioning of the potential energy to C_2H_4 vibration energy is negligible, in contrast to the large partitioning inferred from the summary of incomplete experimental data from several systems.

The origin of this difference, between the partitioning of the potential energy release found from the direct dynamics simulations and suggested from experiments for a variety of HX eliminations, is unclear. One possible factor is the assumption made, in summarizing the experiments, that partitionings of the exit-channel potential barrier for different HX eliminations are similar, regardless of the masses of the substituent atoms. For example, the energy released to relative translation for $C_2H_5F \rightarrow HF + C_2H_4$ dissociation was deduced from experiments for $CH_3CCl_3 \rightarrow HCl + C_2H_2Cl_2$ dissociation.[21] As part of an incomplete study, currently in progress, we have found that the masses of the substituent atoms may be important.[22] When the MP2/6-31G* potential for $C_2H_5F \rightarrow HF + C_2H_4$ is used in the direct dynamics simulation, but the atomic masses are changed in calculating the trajectories, the energy partitioning may change. Preliminary results show that changing the mass of F to Cl, to model $C_2H_5Cl \rightarrow HCl + C_2H_4$, has at most a very small effect on the partitioning of the exit-channel potential energy release. However, if the mass of two of the H-atoms are also changed to that for Cl, to model $CH_3CCl_3 \rightarrow HCl + C_2H_4Cl_2$ dissociation, there is a dramatic change in the energy partitioning. The partitioning of the exit-channel barrier to relative translation is lowered to ~45%, while the partitioning to $C_2H_2Cl_2$ vibration and rotation is increased to ~25% and 10%, respectively. Thus, this incomplete study suggests that mass effects, in addition to features of the potential energy surface, are important in interpreting product energy partitioning for HX elimination reactants.

IV. Summary

For the work presented here, MP2/6-311++G** direct dynamics simulations are performed to determine product energy partitioning for $C_2H_5F \rightarrow HF + C_2H_4$ dissociation. MP2/6-311++G** theory gives an exit-channel potential with a reverse barrier in excellent agreement with both experiment and the CCSD(T)/6-311++G** calculated barrier. The results of the simulations are compared with experimental studies of the energy partitioning and a previous direct dynamics simulation also using MP2 theory, but the smaller 6-31G* basis set. The larger basis set MP2 calculation gives a more accurate potential energy surface and product energy partitioning in better agreement with experiment.

As shown in Table 4, the fraction of the available energy released to product relative translation decreases and the fraction released to HF vibration increases as the basis set size is increased from 6-31G* to 6-311++G**. The changes in the other energy partitionings are quite small. Equation 4 allows the partitioning of the available energy to a product energy type i to be distinguished between a fraction coming from the potential energy release and another fraction coming from the excess energy at the barrier. Both of these fractions decrease for the relative translation product energy, and both of these fractions increase for HF vibration, when the basis set size is increased. For example, the fractional releases of the potential energy and of the excess energy to HF vibration are 0.11 and 0.046, respectively, for the 6-31G* basis set and 0.18 and 0.11, respectively, for the 6-311++G** basis set.

Differences in the potential energy surfaces for the 6-31G* and 6-311++G** basis sets are expected to lead to differences in their product energy partitioning. As shown in Tables 1 and 2, the two surfaces have similar TS structures, with bond lengths differing by ~0.05 Å or less. The 0.048 Å longer H−F distance for the 6-311++G** TS suggests this surface may partition more energy to HF vibration, as found in the trajectory simulations. Overall, the two basis sets give similar sets of values for the TS vibrational frequencies. The TS imaginary frequencies are 2030i and 1925i for the 6-31G* and 6-311++G** calculations, respectively. However, the values of the CCF and HCC bending frequencies are ~10% smaller for the larger basis set. Also, the 6-311++G** basis set has a 5 kcal/mol larger potential energy release, and its surface releases this potential energy more rapidly in moving from the TS to products than does the 6-31G* basis (see Figure 2 in ref 1). Such differences are expected to affect the potential energy release and may also affect the way the excess energy in the TS is distributed to product energies. However, a statistical model for product energy partitioning assumes the latter is determined by the energy distribution in the TS, which is unperturbed by the dynamics in moving from the TS to products.[14] Thus, the a_i found from eq 4 should be unaffected by the level of theory used for the direct dynamics. The large difference in the a_i for HF vibration, i.e., values of 0.46 and 0.11, is inconsistent with this model. It is possible that this difference arises from statistical

uncertainties in the current simulation, an alteration in the TS energy distribution by the exit-channel dynamics, or a combination of both. This is an issue that needs to be addressed in future work. The product energy partitioning direct dynamics for $C_2H_5F \rightarrow HF + C_2H_4$ could be performed at the HF, B3LYP, and MP2 levels of theory, with a range of basis sets and for large ensembles of trajectories to obtain excellent statistics. It would be of interest to determine possible variations in the set of a_i which fit the simulation results.

Setser and co-workers[3] have measured the populations of HF vibrational states prepared when C_2H_5F dissociates with an excess energy of 42.9 kcal/mol above the dissociation barrier. Their experiments show that 15% of the energy available to the products is partitioned to HF vibration, and the MP2/6-311++G** simulation gives 14% and nearly the same result. In addition, the experimental and simulated populations $P(n)$ of the HF vibrational states n are in very good agreement. Infrared multiple photon absorption (IRMPA) is thought to dissociate C_2H_5F molecules with energies in the range 20−35 kcal/mol and the simulated $P(n)$ distribution for $E_{vt}^{\ddagger} = 32$ kcal/mol is in overall good agreement with experiment. The principal difference between the simulated and experimental distributions is the small $P(1)/P(0)$ inversion found from the simulations. The temperature of the HF rotational states has been estimated in the IRMPA experiments, and the MP2 simulated $P(J)$ distribution, for both the 6-31G* and 6-311++G** basis set, is in good agreement with experiment after the effect of collisional relaxations in the experiments are taken into account.

From an analysis of the product energy partitioning versus the energy of C_2H_5F in excess of the dissociation barrier, the manner in which the exit-channel potential energy barrier is released to the products was determined from the simulations. The MP2 simulations, with both the 6-31G* and 6-311++G** basis sets, distribute the vast majority of this potential energy release to the $HF + C_2H_4$ relative translation, i.e., 70−80%, with the HF vibration the next important recipient and receiving 10−20%. The partitioning to C_2H_4 vibration is less than 5% and quite small. These findings are inconsistent with a model proposed to summarize experiments of HX elimination from a variety of haloalkanes. This model proposed that 45% of the potential energy release is partitioned to C_2H_4 vibration, with relative translation receiving a lesser amount of 20%. The origin of this difference between simulation and the model proposed from the experimental studies is unclear. It will be of interest to perform the $C_2H_5F \rightarrow HF + C_2H_4$ simulations at an even higher level of electronic structure theory. Also, it would be useful to investigate the applicability of the model used to summarize the HX elimination experimental data. This model assumes similar energy partitioning dynamics for HX eliminations which have different atoms and/or groups attached to the halo-carbon, e.g., C_2H_5F and CH_3CCl_3. In an incomplete study of the effect of mass on HX elimination product energy partitioning,[22] it was found that simulations of $C_2H_5F \rightarrow HF + C_2H_4$ and $CH_3CCl_3 \rightarrow HCl + C_2H_2Cl_2$ dissociation gave significantly different product energy distributions, when both simulations are performed on the potential energy surface (PES) for the former reaction. The suggestion from this study is that mass and kinematic effects are important for product energy partitioning, as well as PES properties. Indications of such a mass effect also come from experiments of HF elimination from fluorinated alkanes. The rotational temperatures for HF elimination are higher for CH_3CHF_2 and CH_3CF_3 than for C_2H_5F.[3] Mass effects for HX elimination from haloalkanes need to be investigated in more detail in future work.

Acknowledgment. This research is based on work supported by the National Science Foundation under grant no. 0412677 and the Robert A. Welch Foundation. The authors wish to thank Dr. Lipeng Sun for many helpful discussions concerning the dynamics of HX elimination from haloalkanes.

Note Added after ASAP Publication. This article was published ASAP on September 13, 2005. A correction was made in the caption of Figure 3. The correct version was reposted on December 19, 2005.

References and Notes

(1) Sun, L.; Hase, W. L. *J. Chem. Phys.* **2004**, *121*, 8831.
(2) Quick, C. R., Jr.; Wittig, C. *J. Chem. Phys.* **1980**, *72*, 1694.
(3) Arunan, E.; Wategaonkar, S. J.; Setser, D. W. *J. Phys. Chem.* **1991**, *95*, 1539.
(4) Pioneering discussions of product energy partitioning associated with HF elimination from haloalkanes are given in Chang, H. W.; Setser, D. W.; Perona, M. J. *J. Phys. Chem.* **1972**, *76*, 954.
(5) Frisch, M. J.; Trucks, G. W.; Schlegel, H. B.; Scuseria, G. E.; Robb, M. A.; Cheeseman, J. R.; Montgomery, J. A., Jr.; Vreven, T.; Kudin, K. N.; Burant, J. C.; Millam, J. M.; Iyengar, S. S.; Tomasi, J.; Barone, V.; Mennucci, B.; Cossi, M.; Scalmani, G.; Rega, N.; Petersson, G. A.; Nakatsuji, H.; Hada, M.; Ehara, M.; Toyota, K.; Fukuda, R.; Hasegawa, J.; Ishida, M.; Nakajima, T.; Honda, Y.; Kitao, O.; Nakai, H.; Klene, M.; Li, X.; Knox, J. E.; Hratchian, H. P.; Cross, J. B.; Bakken, V.; Adamo, C.; Jaramillo, J.; Gomperts, R.; Stratmann, R. E.; Yazyev, O.; Austin, A. J.; Cammi, R.; Pomelli, C.; Ochterski, J. W.; Ayala, P. Y.; Morokuma, K.; Voth, G. A.; Salvador, P.; Dannenberg, J. J.; Zakrzewski, V. G.; Dapprich, S.; Daniels, A. D.; Strain, M. C.; Farkas, O.; Malick, D. K.; Rabuck, A. D.; Raghavachari, K.; Foresman, J. B.; Ortiz, J. V.; Cui, Q.; Baboul, A. G.; Clifford, S.; Cioslowski, J.; Stefanov, B. B.; Liu, G.; Liashenko, A.; Piskorz, P.; Komaromi, I.; Martin, R. L.; Fox, D. J.; Keith, T.; Al-Laham, M. A.; Peng, C. Y.; Nanayakkara, A.; Challacombe, M.; Gill, P. M. W.; Johnson, B.; Chen, W.; Wong, M. W.; Gonzalez, C.; Pople, J. A. *Gaussian 03*, revision C.02; Gaussian, Inc.: Wallingford, CT, 2004.
(6) Hase, W. L.; Duchovic, R. J.; Hu, X.; Komornicki, A.; Lim, K. F.; Lu, D.-h.; Peslherbe, G. H.; Swamy, K. N.; Vande Linde, S. R.; Varandas, A.; Wang, H.; Wolf, R. J. *QCPE Bull.* **1996**, *16*, 671.
(7) Baer, T.; Hase, W. L. *Unimolecular Reaction Dynamics. Theory and Experiments*; Oxford: New York, 1996; p 364.
(8) Hase, W. L.; Buckowski, D. G. *Chem. Phys. Lett.* **1980**, *74*, 284.
(9) Doubleday, C., Jr.; Bolton, K.; Peslherbe, G. H.; Hase, W. L. *J. Am. Chem. Soc.* **1996**, *118*, 9922.
(10) Gutzwiller, M. C. *Chaos in Classical and Quantum Mechanics*; Springer: New York, 1990.
(11) Polanyi, J. C.; Wong, W. H. *J. Chem. Phys.* **1969**, *51*, 1439.
(12) Levine, R. D.; Bernstein, R. B. *Molecular Reaction Dynamics and Chemical Reactivity*; Oxford: New York, 1987; p 155.
(13) Zamir, E.; Levine, R. D. *Chem. Phys.* **1980**, *52*, 253.
(14) Holmes, B. E.; Setser, D. W. *J. Phys. Chem.* **1978**, *82*, 2450.
(15) Hase, W. L.; Bhalla, K. C. *J. Chem. Phys.* **1981**, *75*, 2807.
(16) Wang, H.; Hase, W. L. *J. Am. Chem. Soc.* **1997**, *119*, 3093.
(17) Chesnavich, W. J.; Bowers, M. T. In *Gas-Phase Ion Chemistry*; Bowers, M. T., Ed.; Academic: New York, 1979; Vol. 1, p 119.
(18) Marcus, R. A. *J. Chem. Phys.* **1986**, *85*, 1562.
(19) Sirkin, E. R.; Berry, M. J. *IEEE J. Quantum Electron.* **1974**, *QE-10*, 701.
(20) Berry, M. J. In *Molecular Energy Transfer*; Levine, R. D., Jorter, J., Eds.; Wiley: New York, 1976; p 114.
(21) Sudbo, A. S.; Schultz, P. A.; Shen, Y. R.; Lee, Y. T. *J. Chem. Phys.* **1978**, *69*, 2312.
(22) Sun, L.; Song, K.; Setser, D. W.; Hase, W. L. To be published.